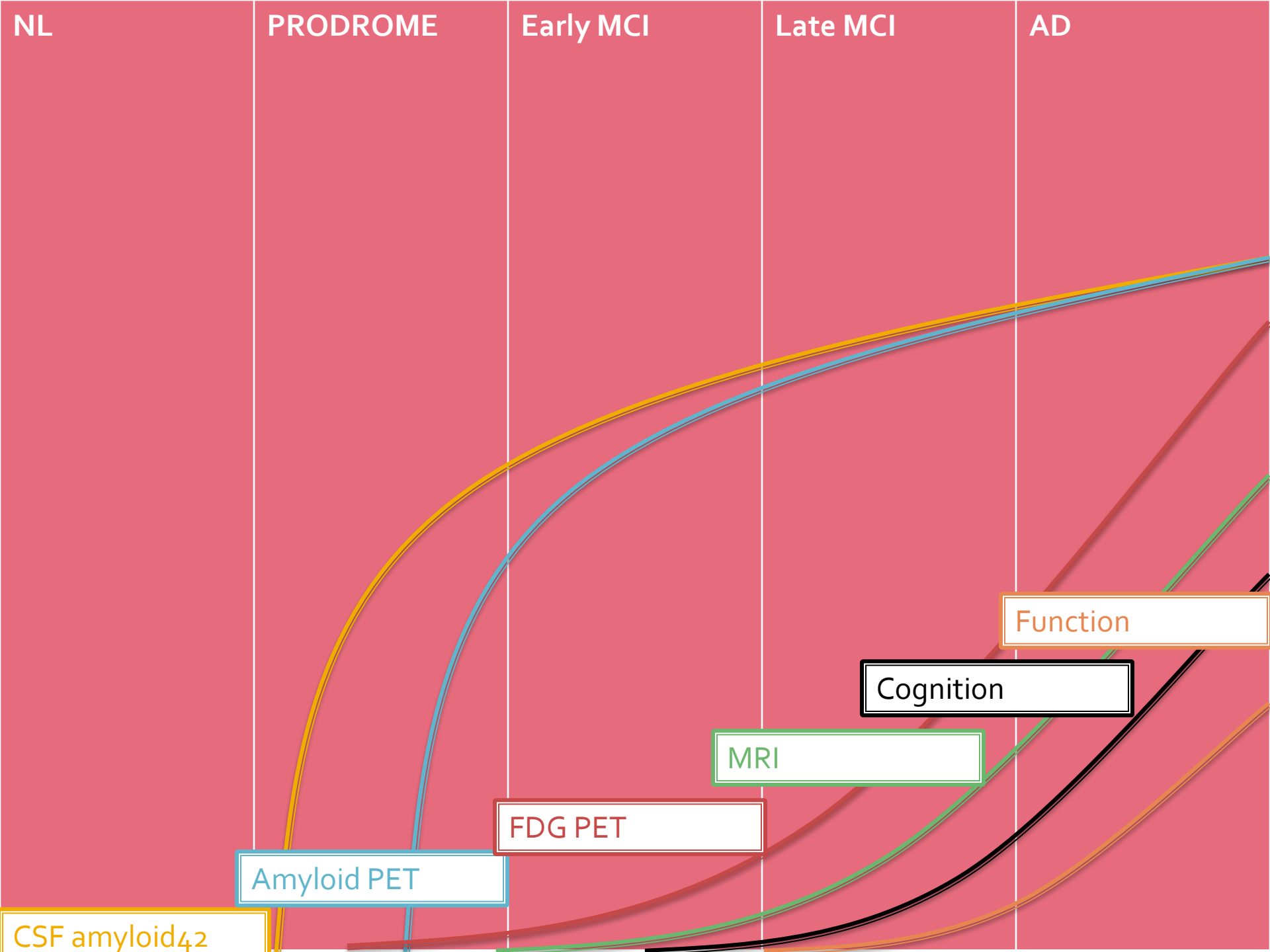


Junyoung Lee, 2011년 11월 25일, 한국노년신경정신약물학회

신경영상기법의 발전과 진단적 타당도



NL

PRODROME

Early MCI

Late MCI

AD

CSF amyloid₄₂

Amyloid PET

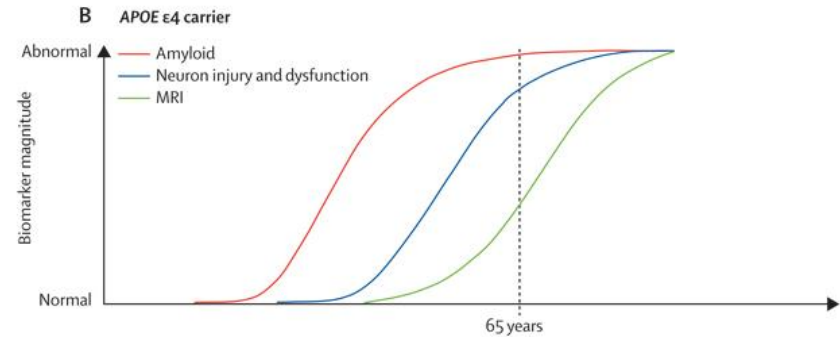
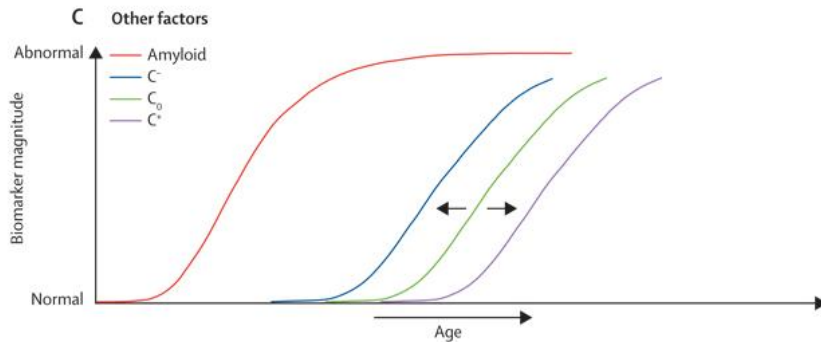
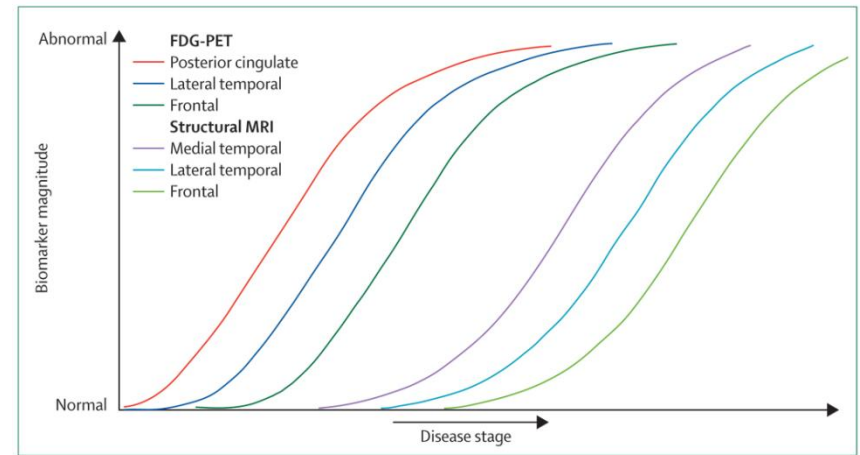
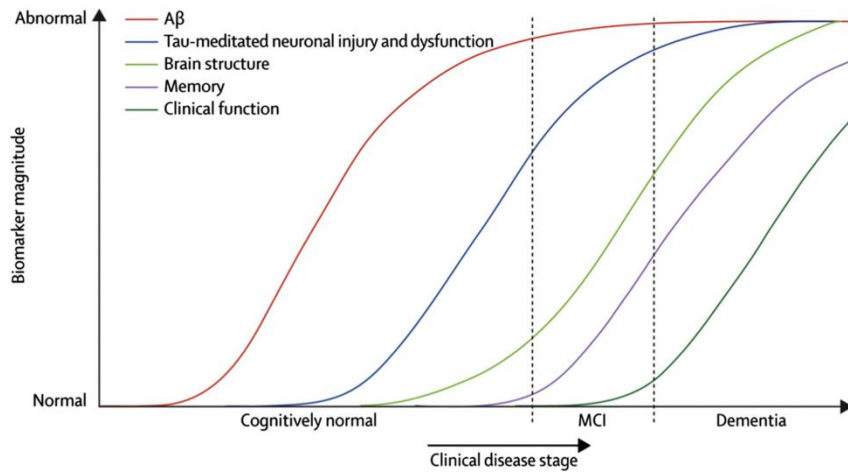
FDG PET

MRI

Cognition

Function

Hypothetical model of biomarkers of AD



MCI and Imaging

Left: Mild cognitive impairment progressor, Top: positive PIB PET. Bottom: MRI illustrating atrophic hippocampi and ventricular enlargement.

Right: Mild cognitive impairment non-progressor. Top: negative PIB PET with non-specific white matter retention but no cortical retention. Bottom: MRI illustrating normal hippocampi and no ventricular enlargement (Jack et al, 2010c)

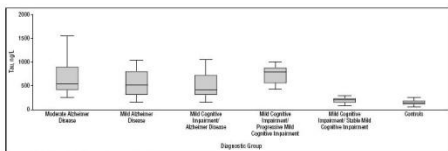
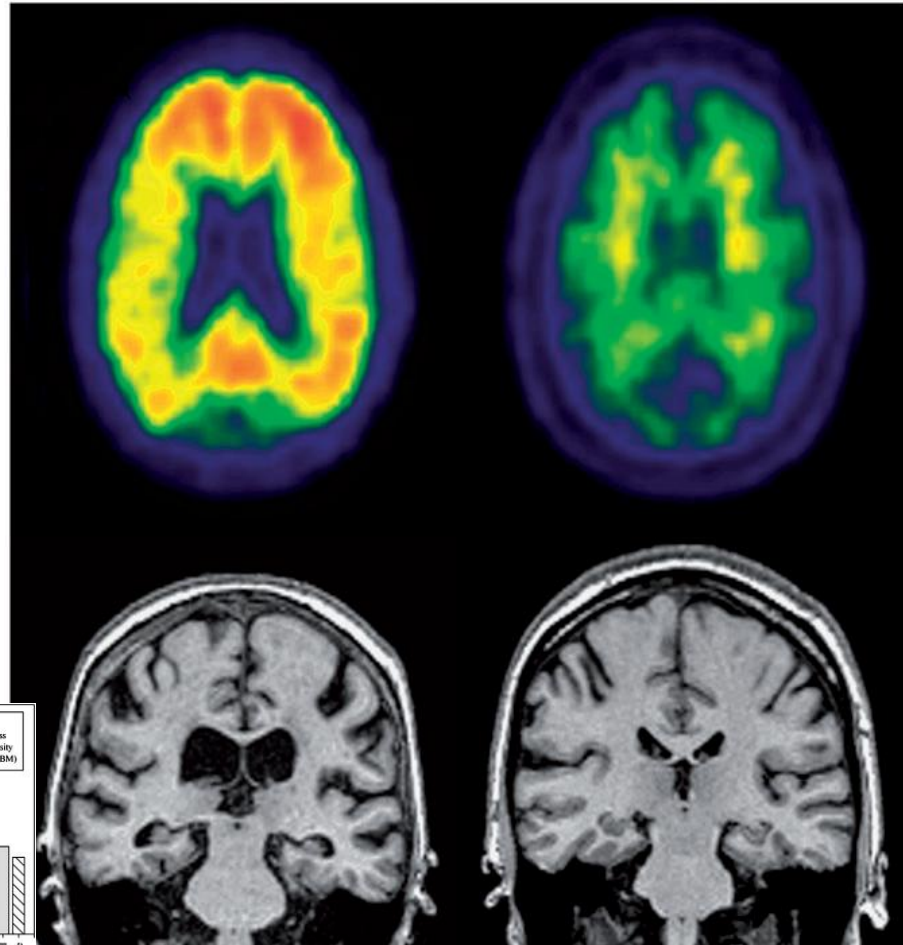


Figure 1. Cerebrospinal fluid tau level by diagnostic group.

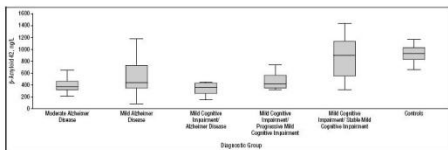
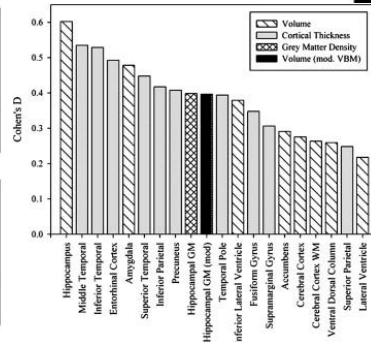
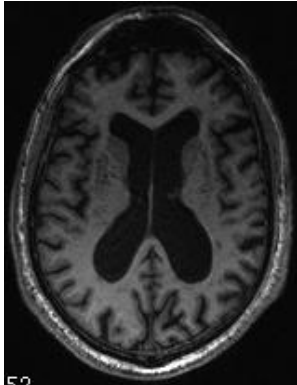


Figure 2. Cerebrospinal fluid p-amyloid 42 level by diagnostic group.

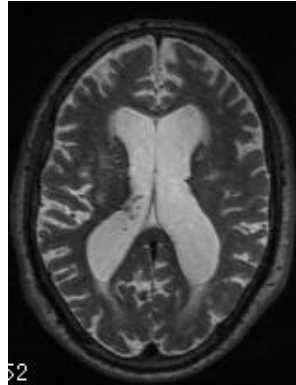


Imaging Modalities

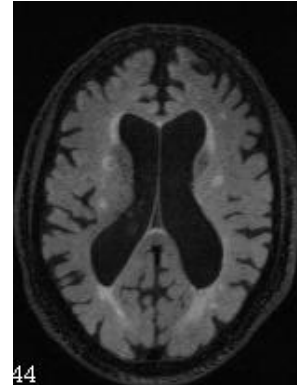
Structural imaging



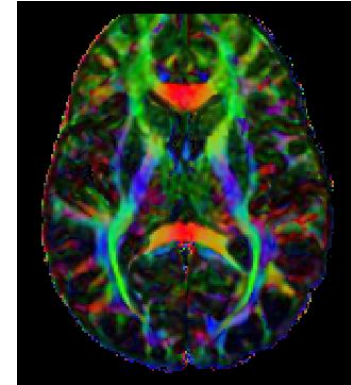
T₁ weighted MRI



T₂ weighted MRI

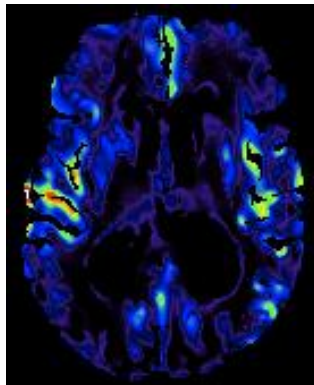


FLAIR MRI

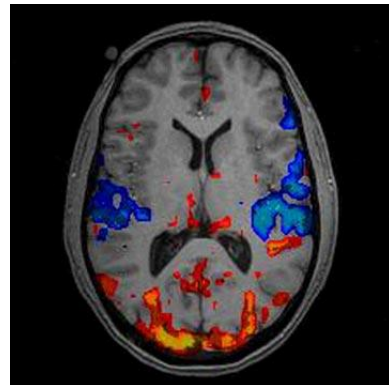


Diffusion weighted MRI

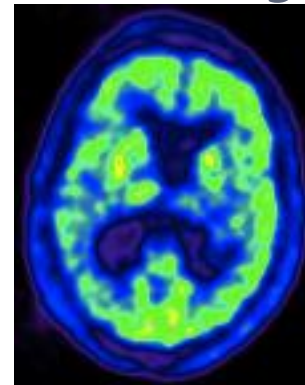
Functional/metabolic imaging



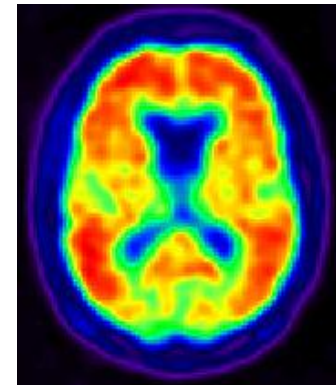
ASL MRI



fMRI

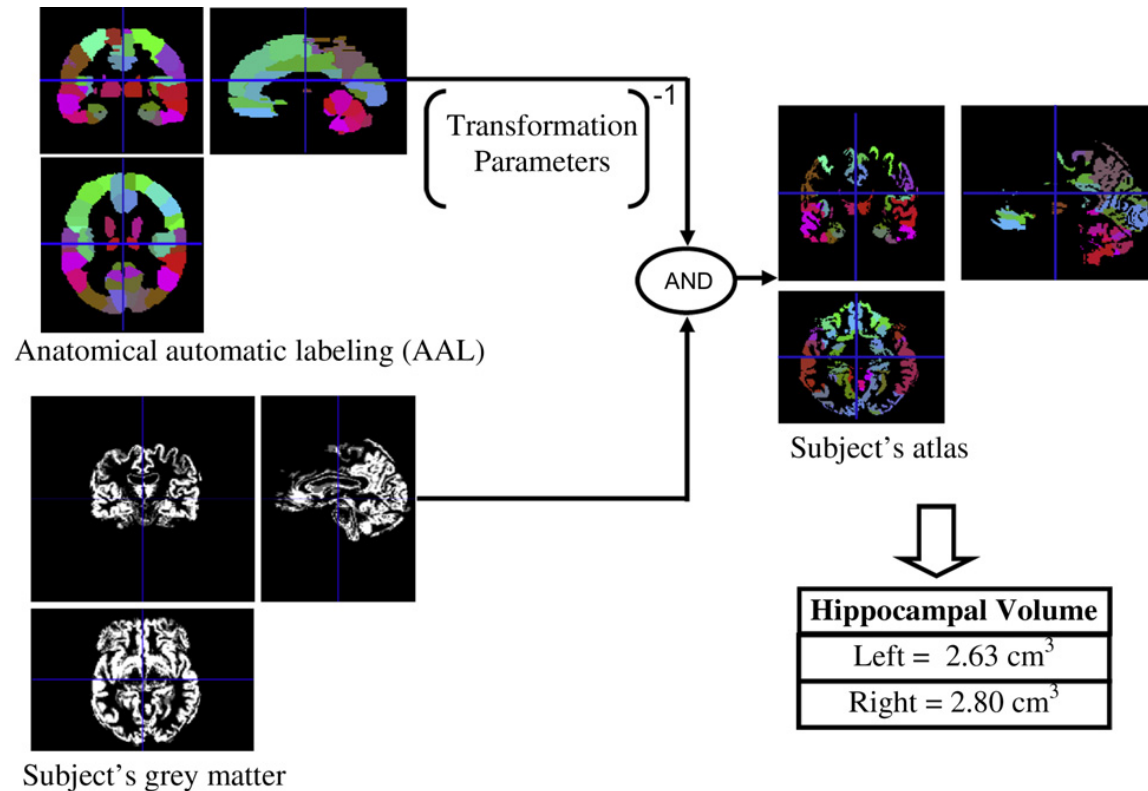


FDG PET



¹¹C-PiB PET

Automated HC volumes

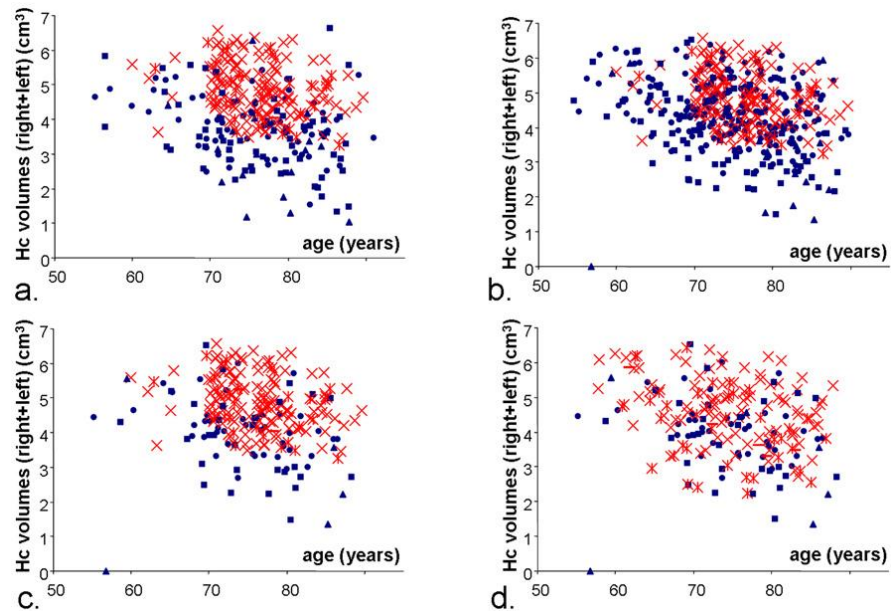


By warping the intensity-coded anatomical automatic labeling (AAL) into the individual subject's grey matter based on the transformation parameters, the individual subject's atlas was obtained. Then hippocampal volumes were calculated by summing the number of voxel of hippocampus in individual subject's atlas and multiply with the voxel size.

Automated HC Volumes

Automatically computed volumes corresponding to the classification experiments: a: CN (red crosses) and AD, b. CN (red crosses) and MCI, c. CN at 18 months (red crosses) and MCI converting at 18 months, d. MCI not converting (red crosses)

Chupin M, [Hippocampus. 2009 June; 19\(6\): 579–587.](#)



AD vs CN	MCI vs CN	MCIc vs CN	MCIc vs CN	MCIc vs MCIc
MMSE	-20% ^{***}	-7% ^{***}	-10% ^{***}	-4% ^{**}
Hc volume (cm ³)	1.80 vs 2.46	2.16 vs 2.46	1.95 vs 2.47	1.95 vs 2.28
Mean Vol. reduct	-27% ^{***}	-12% ^{***}	-21%^{***}	-14% ^{**}
Class. Rate	80%	63%	74%	67%
Sensitivity	80%	63%	75%	65%
Specificity	79%	63%	74%	68%
Threshold (cm ³)	2.13	2.31	2.22	2.12

VRS-MTA

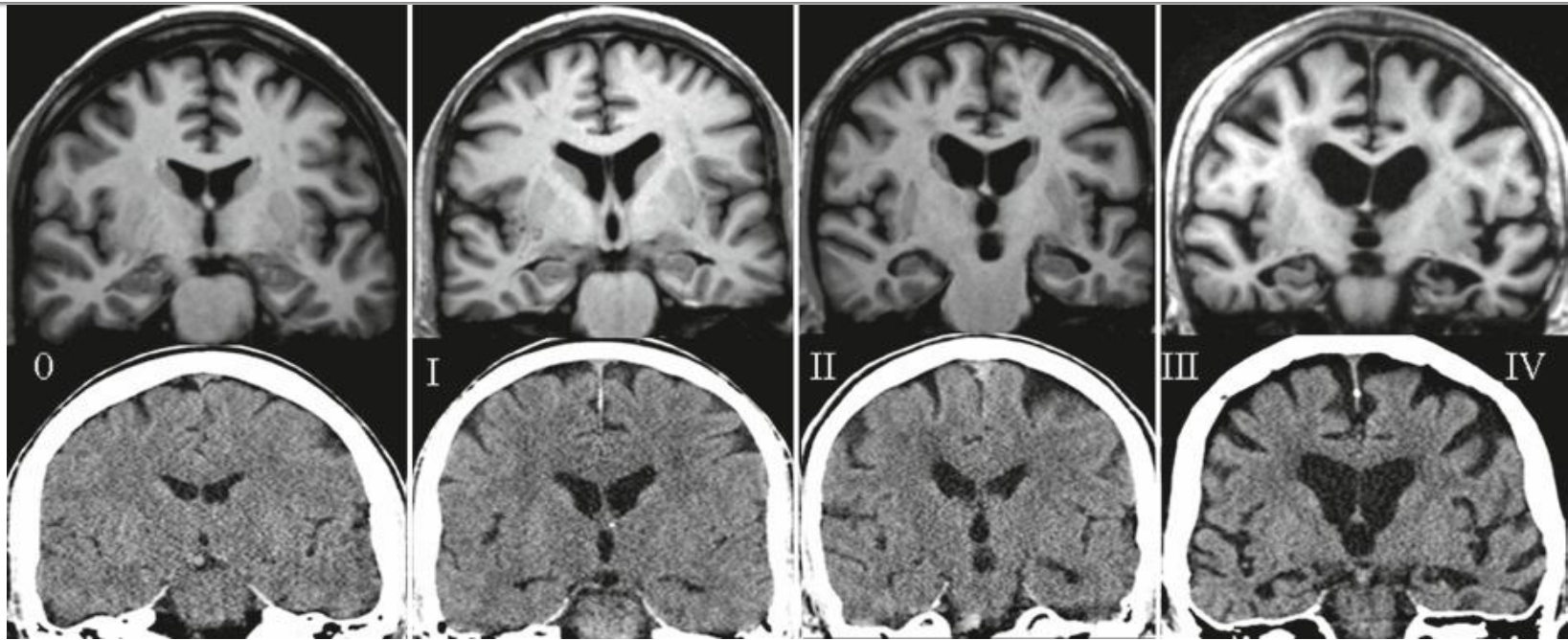


Table 3.5 Visual assessment of medial temporal lobe atrophy (MTA)

Score	Width of choroid fissure	Width of temporal horn	Height of hippocampus
0	N	N	N
1	↑	N	N
2	↑↑	↑	↓
3	↑↑↑	↑↑	↓↓
4	↑↑↑	↑↑↑	↓↓↓

Source: According to Scheltens et al. (1992)

Scheltens (1992) JNNP

↑ increase, ↓ decrease, N normal

VRS-MTA

Comparison of right VRS-MTA to right HPC-Volume AUC values is significantly different at $P = .021$ level.

Q. Shen et al. / Alzheimer's & Dementia 7 (2011)

Table 5

Comparison of areas under the curve (AUC) HPC-volume for distinguishing aMCI from NCI

	AUC	SE	95% CI
HPC-volume left	0.753	0.037	0.682–0.814
VRS-MTA left	0.819	0.032	0.754–0.873
HPC-Volume right	0.725	0.040	0.653–0.789
VRS-MTA right	0.806	0.034	0.740–0.862

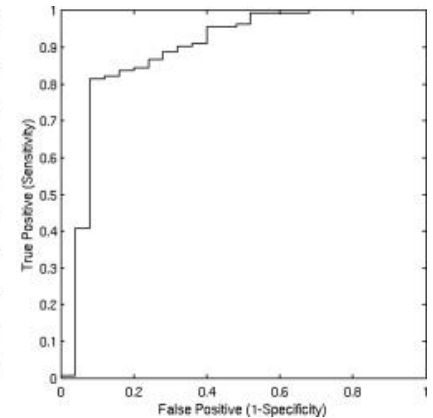
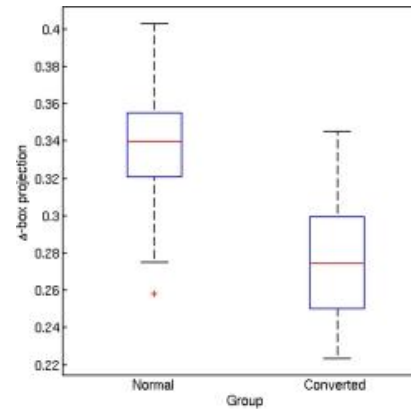
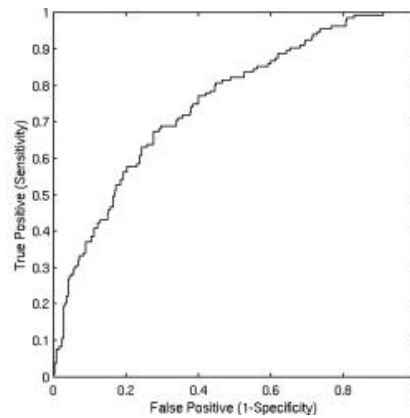
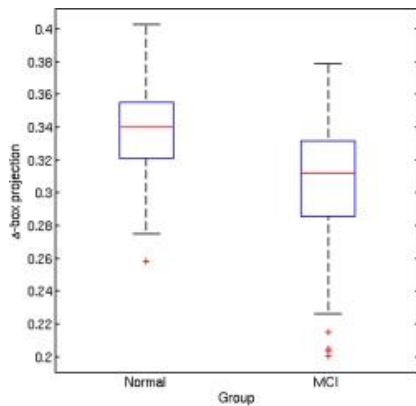
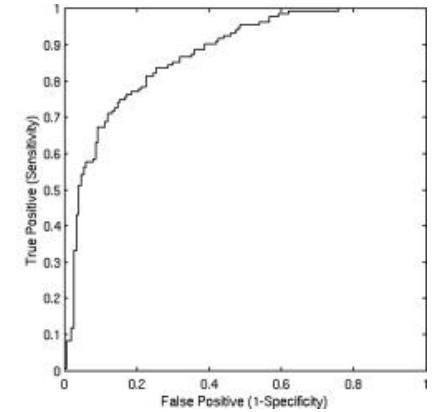
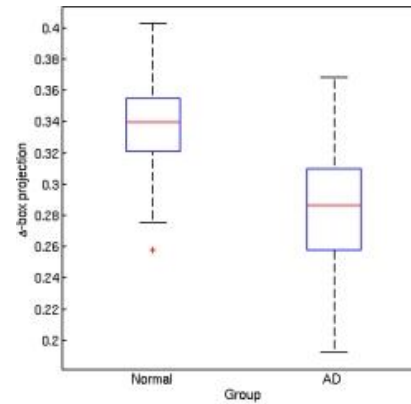
NOTE. Comparison of right VRS-MTA to right HPC-Volume AUC values is significantly different at $P = .021$ level.

Table 2

Volumetric and VRS-MTA scores in different diagnostic groups

	NCI (n = 104)	aMCI (n = 72)	AD (n = 48)	F values
HPC-left volume (SD) [95% CI]	0.20 ^a (0.03) [0.20–0.21]	0.18 ^b (0.03) [0.17–0.18]	0.15 ^c (0.03) [0.15–0.16]	50.17***
HPC-right volume (SD) [95% CI]	0.19 ^a (0.03) [0.18–0.19]	0.16 ^b (0.03) [1.5–1.7]	0.15 ^b (0.04) [0.13–0.16]	27.72***
VRS-MTA-left (SD) [95% CI]	0.45 ^a (0.53) [0.35–0.56]	1.31 ^b (0.84) [1.12–1.51]	2.12 ^c (1.10) [1.80–2.44]	78.80***
VRS-MTA-right (SD) [95% CI]	0.48 ^a (.55) [0.38–.59]	1.38 ^b (.89) [1.173–1.59]	2.01 ^c (1.10) [1.69–2.33]	64.74***

Hippocampal boxes

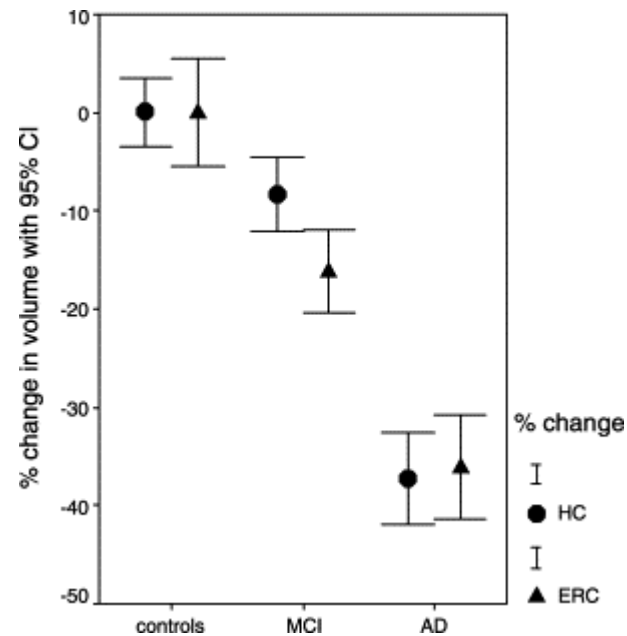


Calvini P, Med Phys. 2009 August; 36(8)

The area under the ROC curve is 88%.

Fig. 1.
Percentual decrease in volume compared to normal mean volumes of ERC and HC in controls, MCI subjects and AD patients. The 95% CI is considered. This figure shows that the most severe volume loss is the ERC in MCI, while in AD there is no significant difference in the magnitude of the volume loss of the two regions of brain

Pennanen C,
[Neurobiology of Aging](#)
[Volume 25, Issue 3](#)



EC

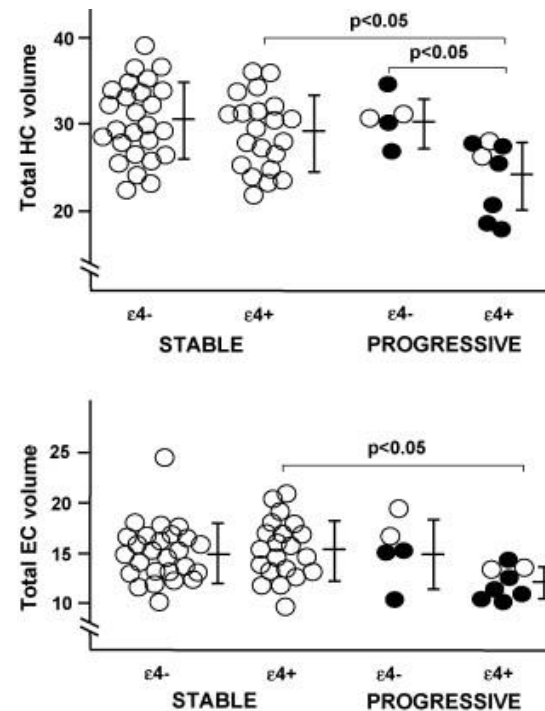
Groups and variables	Sensitivity (%)	Specificity (%)	Overall classific(%)	Explains of variance (%)	P
MCI-C					
Enter: HC	56.9	62.7	59.7	8	0.01
Enter: ERC	63.1	70.7	66.7	16	<0.001
Stepwise: ERC	66.2	65.5	65.9	16	<0.001
AD-C					
Enter: HC	85.4	94.9	90.7	64	<0.001
Enter: ERC	85.4	79.3	82.1	50	<0.001
Stepwise: HC + ERC	87.6	93.1	90.6	66	<0.001
AD-MCI					
Enter: HC	77.1	83.1	80.5	48	<0.001
Enter: ERC	70.8	70.8	70.8	27	<0.001
Stepwise: HC	81.3	83.1	82.3	47	<0.001

EC and conversion

60 subjects with MCI aged 63–81 years. The study subjects were derived from large, population-based random samples of persons living in Kuopio region, Eastern Finland

Fig. 1. Total volumes of the hippocampi and entorhinal cortices in stable and progressive MCI in subjects with at least one APOE ϵ_4 allele or without ϵ_4 allele. Filled circles represent patients with conversion of MCI to AD during the follow-up period.

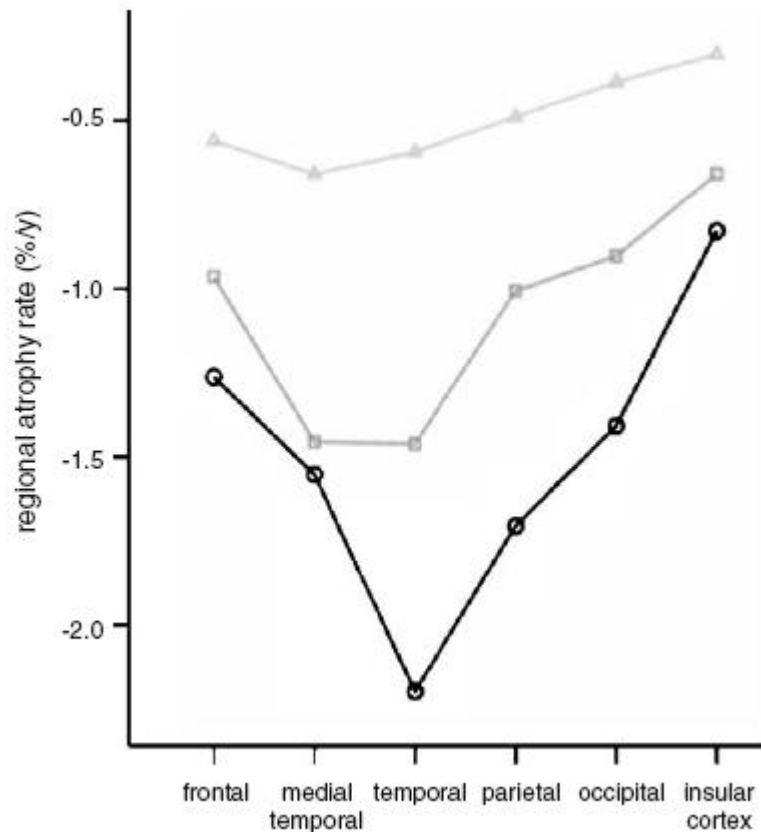
Tapiola T,
[Neurobiology of Aging](#)
[Volume 29, Issue 1](#)



RR: HC 0.731 (0.52–1.03) vs. EC 0.448 (0.24–0.83)

HC Atrophy

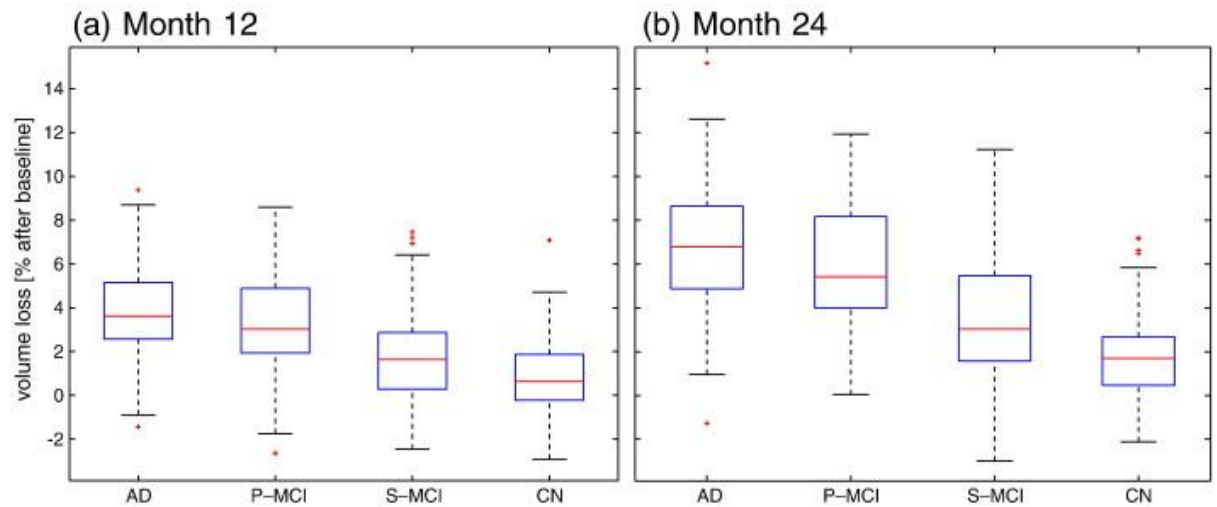
Fig. 2 Regional atrophy rate in six predefined lobar regions are presented by diagnostic group: frontal, medial temporal (hippocampus, amygdala, parahippocampal gyrus), temporal (extramedial), parietal, occipital and insular lobe. In controls, atrophy rates are around 0.5%/year for each region. In MCI patients, atrophy rates start to accelerate mainly in the medial temporal, and remaining temporal lobe (extramedial), and to a lesser extent in the other regions. AD is characterised by a further increase in atrophy rate in the remainder of the temporal lobe, parietal, frontal, occipital and insular lobe. Medial temporal lobe atrophy rates appear to be at a maximum, in the preclinical stage, since the rate is comparable to that of MCI patients. Δ = controls (light grey line); \square = MCI (dark grey line); \circ = AD (black line)



HC atrophy

Fig. 2.
Hippocampal volume loss in %
from Baseline after 12 and 24
months. Box-and whisker plots
for AD, P-MCI, S-MCI, CN.

Wolz R, NeuroImage
Volume 52, Issue 1, 1 August
2010, Pages 109-118



	AD/CN	MCI/CN	P-MCI/CN	P-MCI/S-MCI
Class. rate	82%(86%)	63%(72%)	76%(83%)	66%(67%)
Sensitivity	81%(85%)	59%(65%)	73%(79%)	62%(66%)
Specificity	83%(87%)	71%(83%)	78%(85%)	68%(69%)

HC

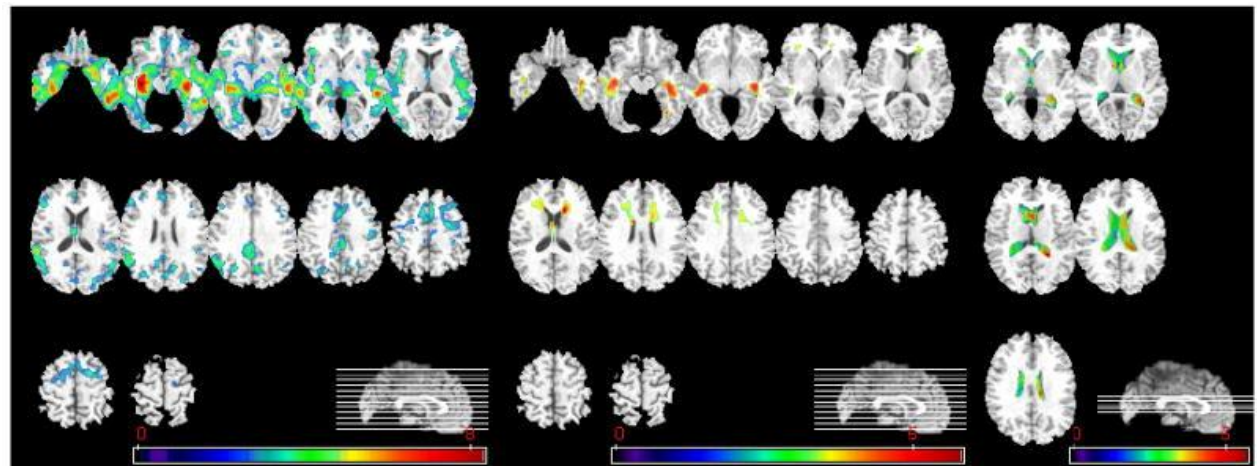
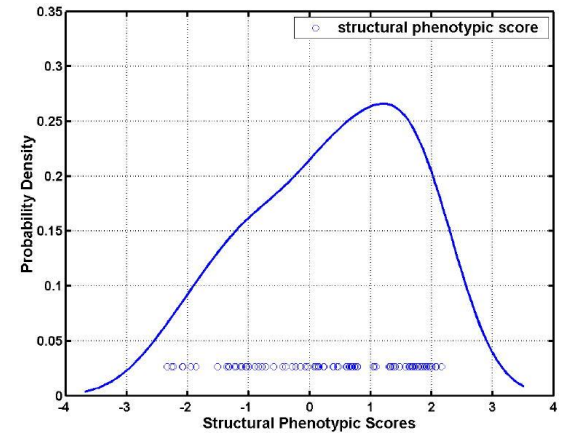
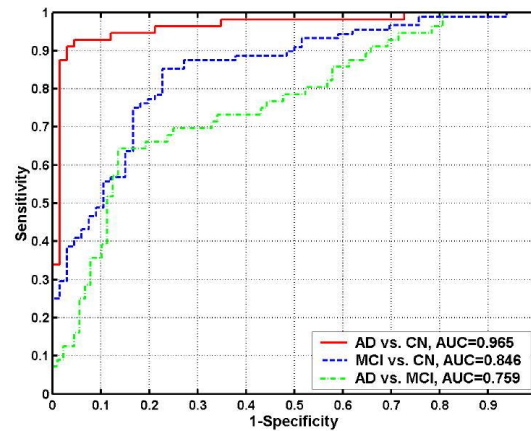
	AD				MCI				MCIc	MCIc			Ref
	Se	Sp	Ac	ROC	Se	Sp	Ac	ROC	Se	Sp	Ac	ROC	
vHC	75	77	76		61	71	72		66	60			68
aHC	81	83	82	0.88	59	71	63	0.71	62	68	66		60
MTL	74	85		0.86	45	85		0.75	85*	83		0.88	66

Pattern classification

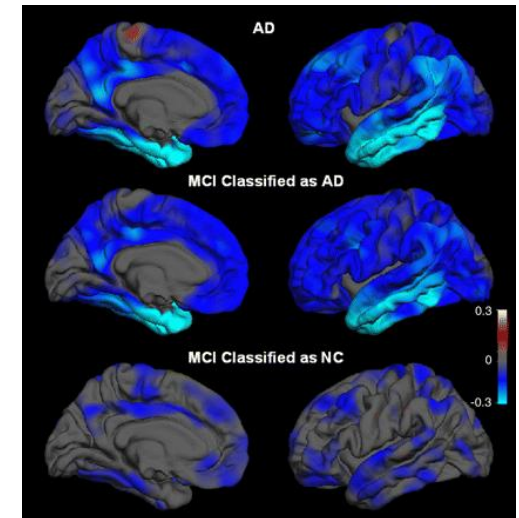
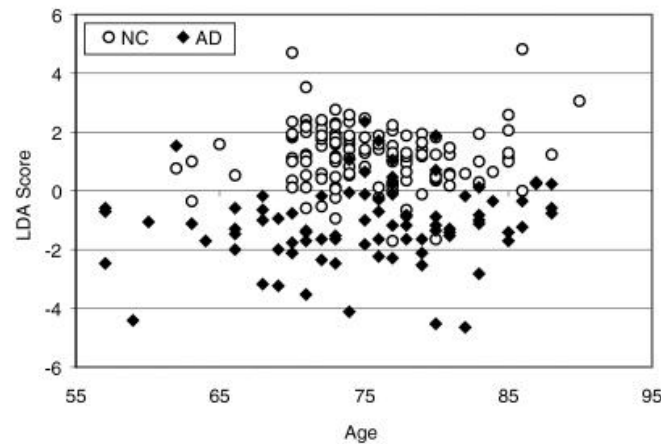
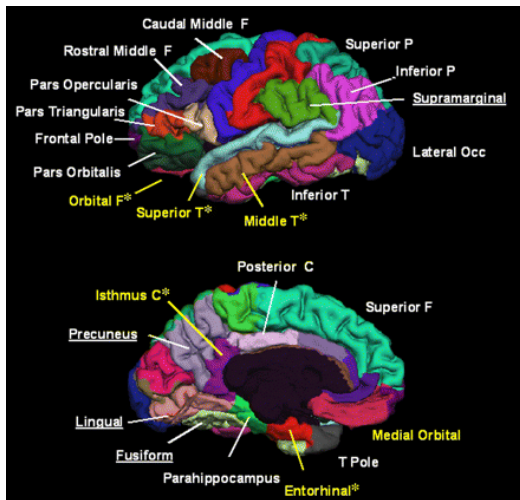
structural phenotypic score (SPS)
individual-patient analysis, aiming to classify individual scans belonging to CN, MCI, or AD participants rather than determining statistical group differences. These include temporal, cingulate, and orbitofrontal regions.

Optimal classification rate of $0.87=87\%$ (AUC 0.86)
Classification rates and areas under the ROC curve obtained by subgrouping MCI patients into progressors and non-progressors

[Neuroimage. 2008 February 15; 39\(4\): 1731-1743](#)
Fan Y



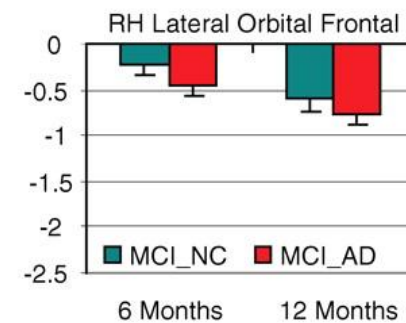
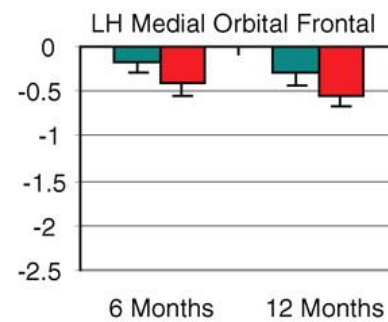
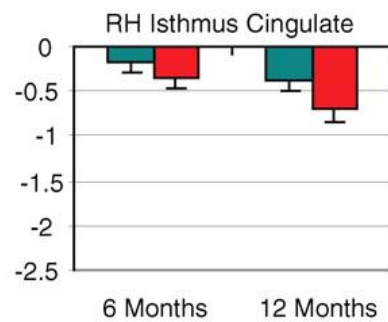
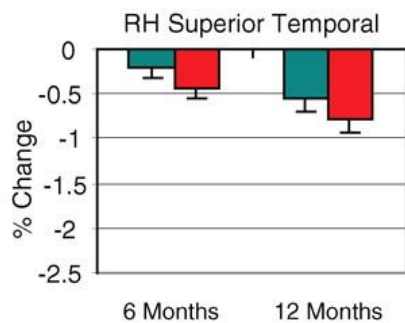
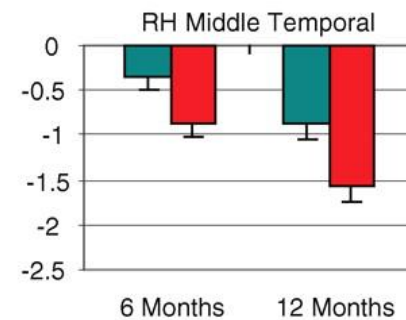
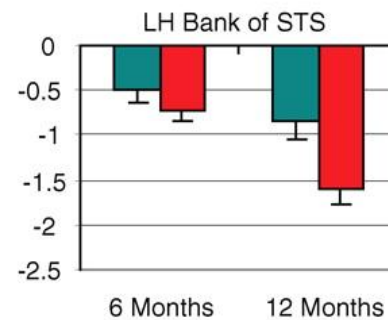
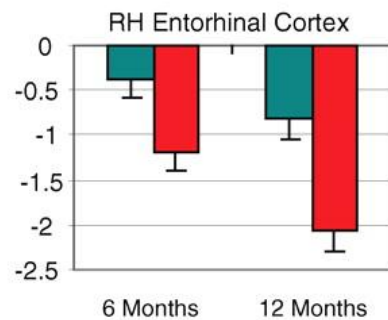
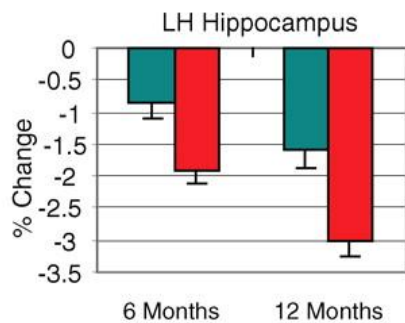
Stepwise linear discriminant analysis



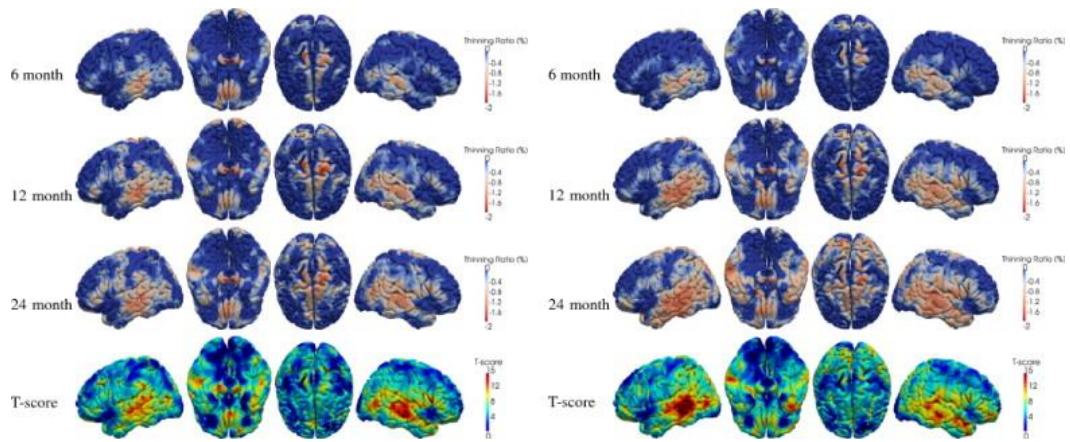
Model	Overall Accuracy (<i>n</i> = 223)*	Sensitivity (<i>n</i> = 84)*	Specificity (<i>n</i> = 139)*	Area under the Curve†
Partially cross validated	92 (205)	89 (75)	94 (130)	0.968 ± 0.011
95% Confidence interval	87.3, 95.0	80.2, 95.3	87.7, 97.2	0.947, 0.989
Fully cross validated	89 (199)	83 (70)	93 (129)	0.915 ± 0.022‡
95% Confidence interval	84.2, 92.8	72.9, 90.5	87.1, 96.8	0.872, 0.958

McEvoy EK, 2009 Radiology, 251

Atrophy in mesial and lateral temporal, isthmus cingulate, and orbitofrontal areas

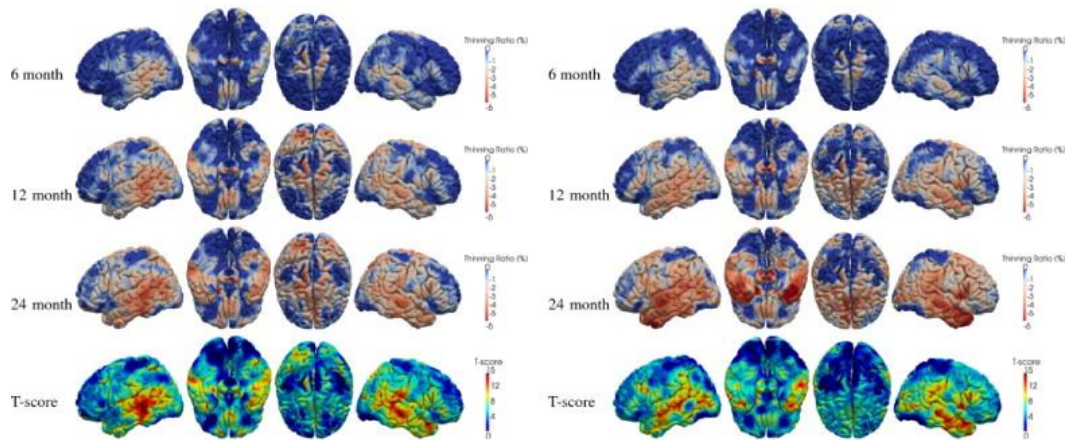


■ MCI_NC ■ MCI_AD



(a) NC

(b) S-MCI



(c) P-MCI

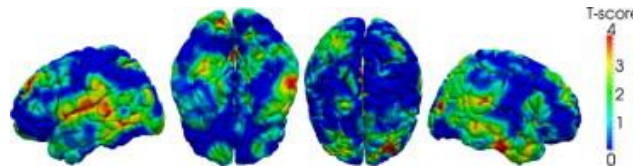
(d) AD

Cortical thinning

Fig. 5. Cortical areas with higher thinning speed in P-MCI group than in S-MCI group. From left to right, T-scores ($p < 0.05$, FDR-corrected) are shown in left, inferior, superior and right views, respectively. parahippocampal cortex, temporal lobe and supramarginal gyrus are found among the regions with high correlations, since relatively high GM loss was also detected in these regions.

LiY, [Neurobiology of Aging](#)
In Press

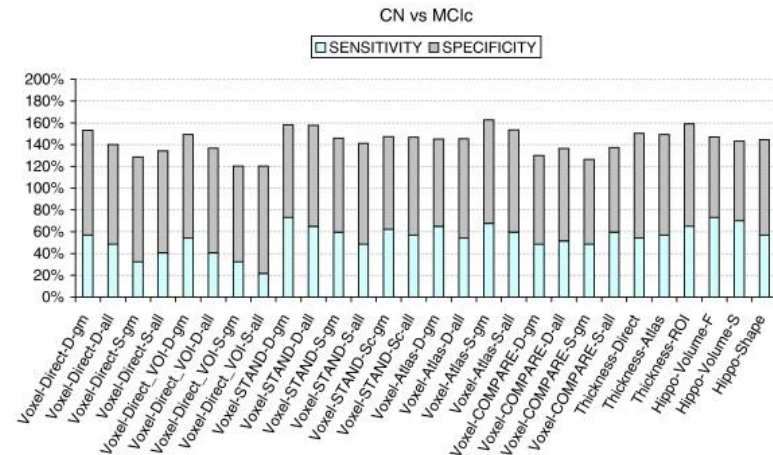
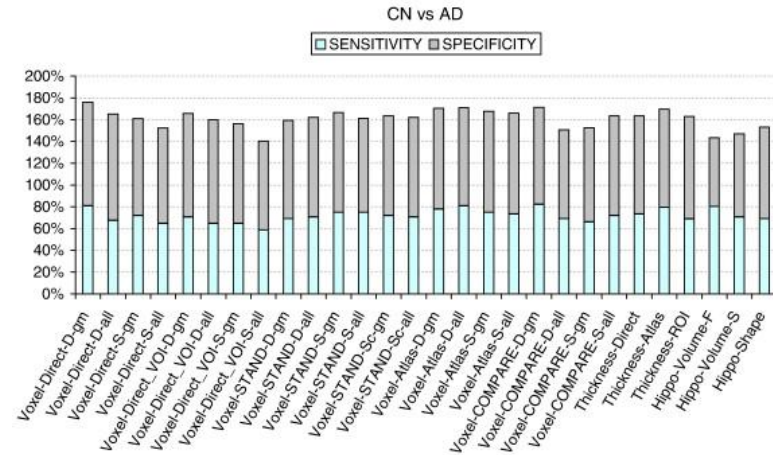
Order	Feature	Regions
(a) AD vs. NC		
1	Endline Thickness	Parahippocampal Left (PHG-L) Fusiform Left (FFG-L)
2	Clustering Coefficient	Olfactory Left (OLF-L)
3	Thinning Speed	Temporal Inferior Right (ITG-R)
4	Endline Thickness	Precentral Right (PreCG-R) Frontal Middle Right (MFG-R)
5	Clustering Coefficient	Cuneus Right (CUN-R)
6	Endline Thickness	Supra Marginal Left (SMG-L) Temporal Supra Left (STG-L)
7	Thinning Speed	Temporal Middle Right (MTG-R) Temporal Inferior Right (ITG-R)
(b) P-MCI vs. S-MCI		
1	Baseline Thickness	Supra Marginal Left (SMG-L) Angular Left (ANG-L) Parietal Inferior Left (IPL-L)
2	Thinning Speed	Postcentral Left (PoCG-L)
3	Thinning Ratio	Temporal Middle Left (MTG-L)
4	Clustering Coefficient	Fusiform Left (FFG-L)
5	Thinning Speed	Paracentral Lobule Left (PCL-L)
6	Thinning Speed	Temporal Middle Right (MTG-R) Temporal Supra Right (STG-R)



Group	Static	Static + dynamic	Static + dynamic + Network
AD vs. NORMAL	89.6%	94.8% (P < 0.0001)	96.1% (P < 0.002)
P-MCI vs. S-MCI	76.7%	80.3% (P < 0.0001)	81.7% (P < 0.003)

Classification results for the different methods.

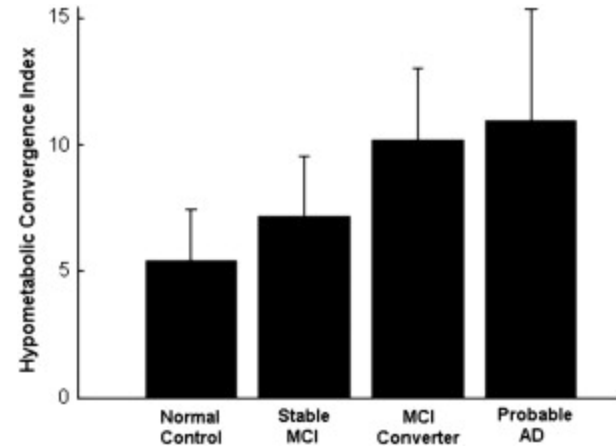
[Neuroimage](#). 2011 May
15;56(2):766-81.
Cuingnet R



FDG-PET

Z_{Pi} is the z-score at voxel i for person P , Z_{Ai} is the z-score at voxel i for AD group (A), and n is the total number of voxels associated with hypometabolism

$$HCI_P = \frac{\sum_{i=1}^n (Z_{Pi} \cdot Z_{Ai})}{10000}$$

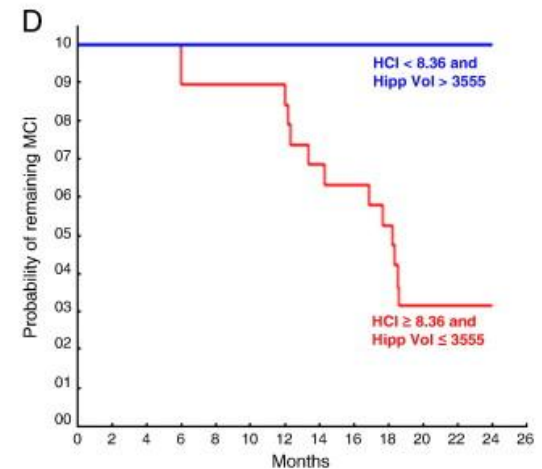
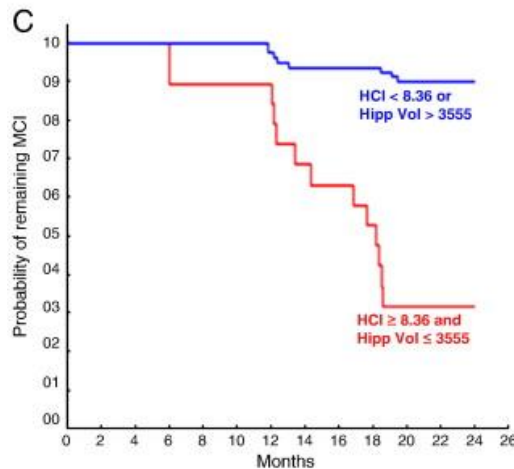
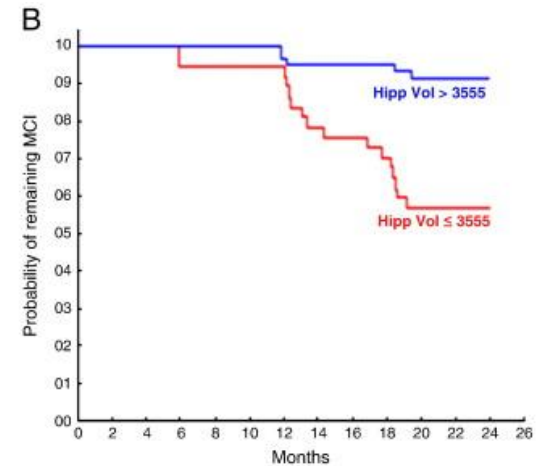
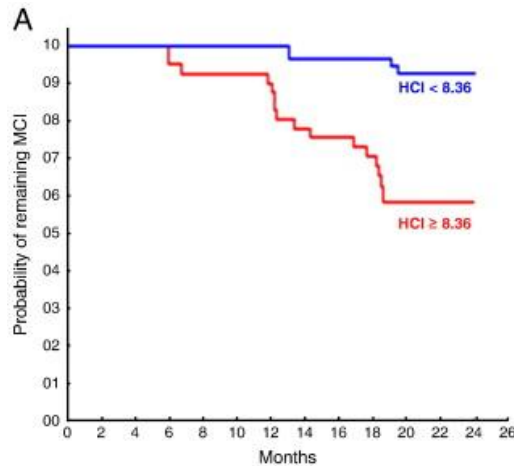


[NeuroImage](#)
[Volume 56, Issue 1](#)
 Chen K

Predictors (MCIs vs. MCIc)	Cut-off values	AUC (95% CI)	Asymptotic significance
ADAS-cog	11.84	0.74 (0.62-0.86)	7.5e-4
CDR-SB	2.25	0.62 (0.47-0.77)	0.11
AVLT-LTM	1.5	0.66 (0.53-0.79)	0.02
HCI	8.36	0.78 (0.68-0.88)	9.4e-5
Hipp volume (mm ³)	3554.72	0.75 (0.64-0.86)	6.0e-4
APOE ε4 carrier status	APOE carrier	0.56 (0.38-0.74)	0.38
CSF			
Aβ ₁₋₄₂	148	0.59 (0.43-0.76)	0.31
p-tau ₁₈₁	32	0.66(0.50-0.82)	0.10
t-tau	81	0.57(0.42-0.72)	0.46
p-tau ₁₈₁ /Aβ ₁₋₄₂	0.23	0.65(0.50-0.80)	0.11
t-tau/Aβ ₁₋₄₂	0.56	0.61(0.45-0.77)	0.27

FDG-PET & HC vol

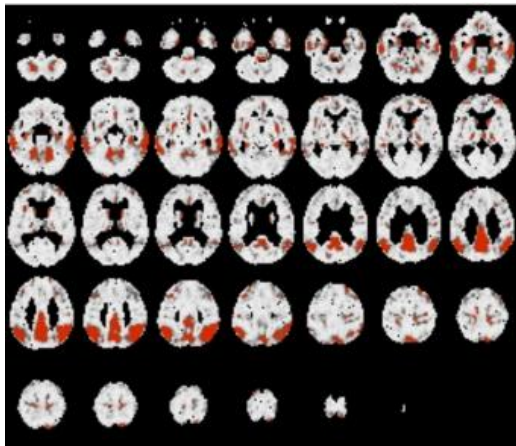
Kaplan–Meier curves showing the probability of an MCI patient not converting to probable AD within 18 months from baseline in (a) the 26 MCI patients with a higher HCl versus the 71 MCI patients with a lower HCl, (b) the 21 MCI patients with a smaller hippocampal volume versus 76 MCI patients with a larger hippocampal volume, and (c) the 20 MCI patients with *both* a higher HCl and smaller hippocampal volume versus the 77 other MCI patients, (d) the 20 MCI patients with *both* a higher HCl and smaller hippocampal volume versus the 38 MCI patients with *both* a lower HCl and larger hippocampal volume.



Feature Selection

Comparison between the performance of the FA proposed in this work and the PCA-based method (PCA) in Ref. 35. m is the number of factors or components.

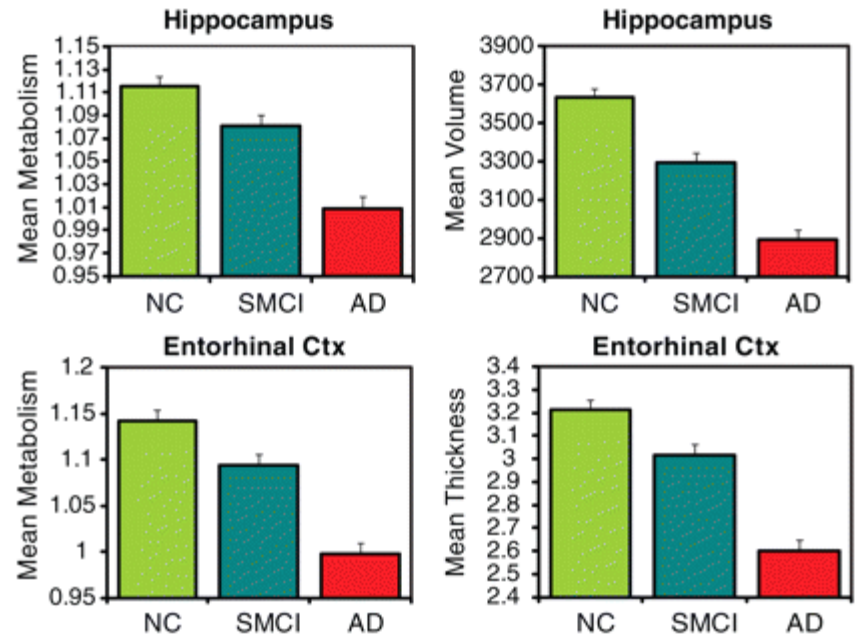
Med Phys. 2010
November; 37(11)
Salaz-Gonzalez



		FA	PCA
NC versus AD	Acc	95.2	89.5
	Sen	98.1	84.5
	Spe	92.5	84.7
	m	17	8
NC versus MCI	Acc	88.0	81.3
	Sen	91.2	97.4
	Spe	80.8	46.1
	m	19	30
NC versus MCI,AD	Acc	86.3	82.2
	Sen	92.8	92.21
	Spe	65.4	50
	m	11	30

Regional PET

September
2010 Radiology, 256, 932-942.
Karow DS



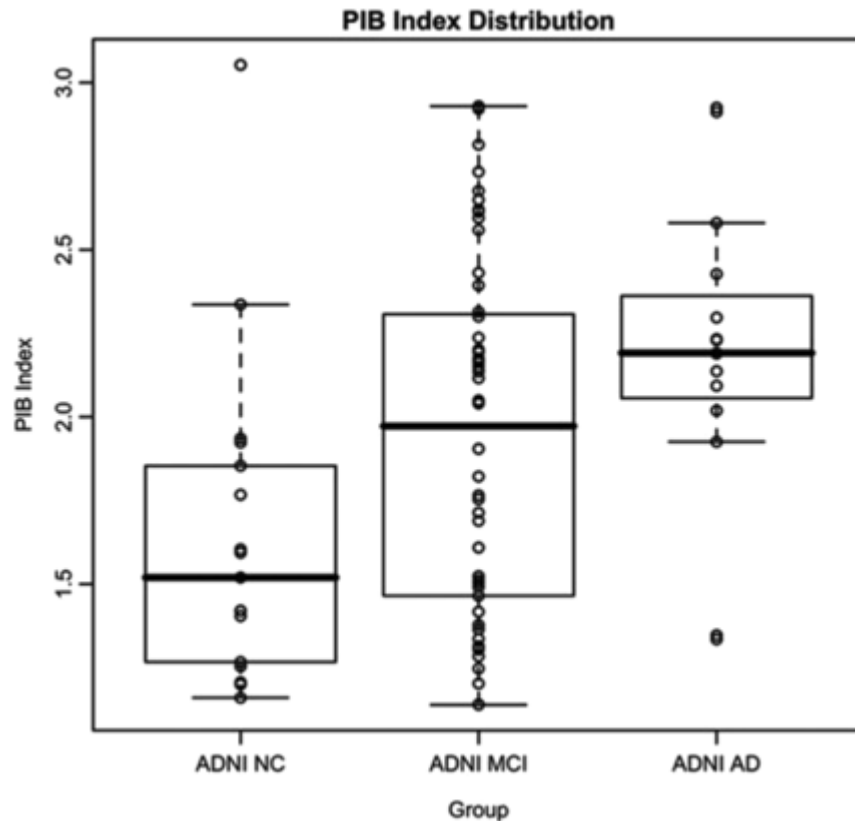
ROI	AUC	Standard Error	CI	P Value, Hippocampus vs Entorhinal Cortex
AD				<.001
Hippocampus (MR imaging)	0.899	0.026	0.847, 0.951	
Entorhinal cortex (FDG PET)	0.706	0.043	0.621, 0.792	
MCI				<.01
Hippocampus (MR imaging)	0.751	0.032	0.689, 0.813	
Entorhinal cortex (FDG PET)	0.626	0.038	0.552, 0.700	
SMCI				<.05
Hippocampus (MR imaging)	0.717	0.043	0.633, 0.801	
Entorhinal cortex (FDG PET)	0.588	0.047	0.496, 0.680	

PIB

Figure 3 Box and whiskers plot showing the distribution of SUVR PIB index values in ADNI groups.

A cut off value of 1.465 optimized discrimination between BAC NC and UCSF Alzheimer's disease subjects (sensitivity of 0.90 and specificity of 0.90 for the diagnosis of Alzheimer's disease) and was selected as the threshold for PIB-positivity. Application of this cut off value to the ADNI MCI cohort stratified 39/52 (75%) MCI subjects as PIB+ and 13/52 (25%) as PIB-. PIB+ MCI subjects were not significantly different from PIB- MCI subjects in age, gender, education, MMSE, aHV or EM ($P > 0.05$).

Mormino EC, Brain (2009) 132 (5)



치매의 생물학적 의미

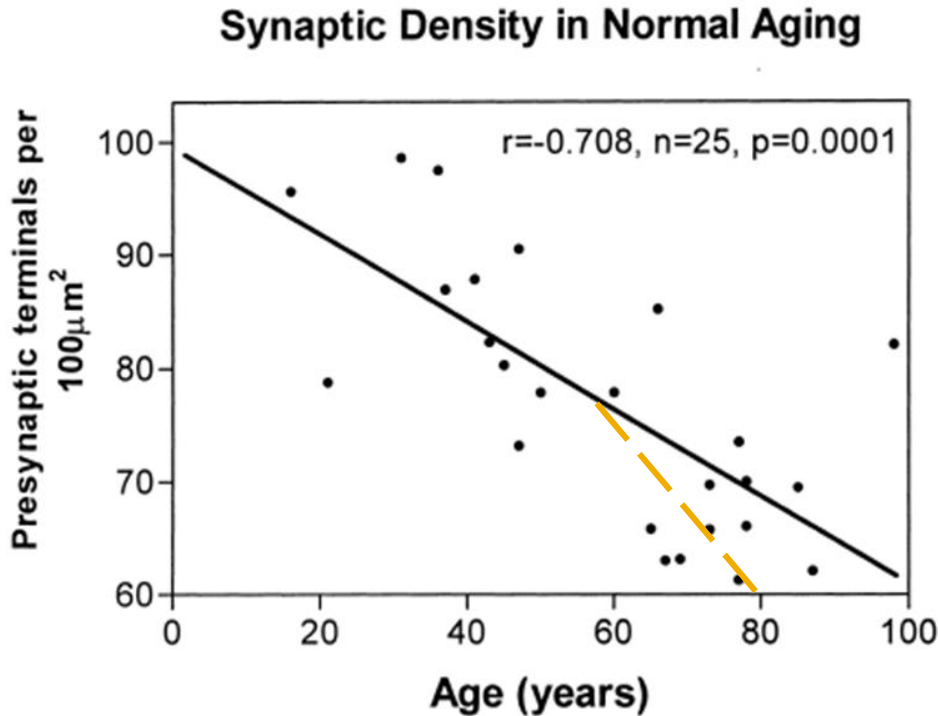


Fig. 1. The density of presynaptic terminals measured by confocal microscopy of vibratome sections of superior prefrontal gyrus reacted with anti-synaptophysin plotted against the patient's age (reference 3). Cognition had been considered to be normal in each case.

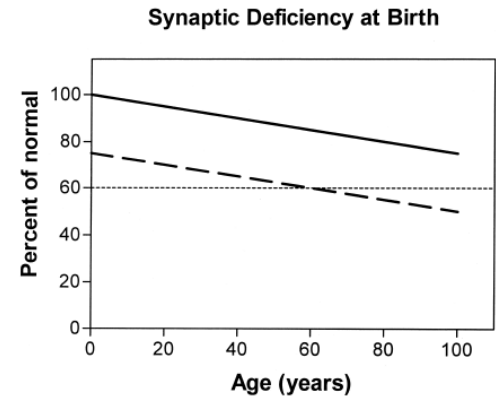


Fig. 2. The dashed line represents a hypothetical group of people born with deficient synapses such that with a normal rate of age-related decline they would cross the 60% threshold significantly earlier than the normals shown in the solid regression line.

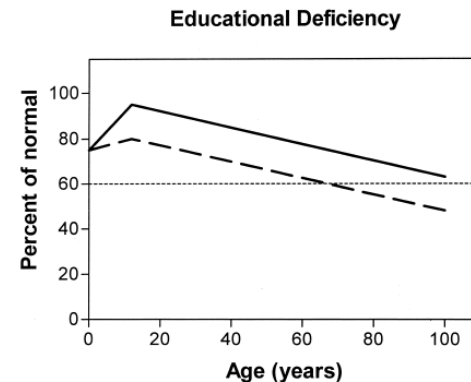


Fig. 3. Education would induce a rapid rise in neocortical synaptic density in the early years of life. Little or no education as seen in the dashed line would result in earlier arrival at the critical 60% threshold.

Combined analysis

Ewers M, 2010, NBA

Table 1. Predictors of models displayed in [Fig. 3](#). AVLT-DEL REC, AVLT delayed free recall; AVLT-IM REC, AVLT immediate free recall; AVLT-DEL RECOG, AVLT recognition memory; BNT, Benton naming test; Cat Fluency (ANI), Category fluency for category of animals; Cat Fluency (VEG), Category fluency for category of vegetables; Digit span B, Digit span backwards (length); Digit span F, Digit span forward (length); Digit Score, Digit span total score; LERC, left entorhinal cortex thickness; LHC, left hippocampus volume; RERC, right entorhinal cortex thickness; LHC, left hippocampus volume; TMT-A, Trail Making Test A; TMT-B, Train Making Test B.

Rank	Single predictor	2-predictor model	3-predictor model	4-predictor model
1	RERC	LHC digit span	LHC LRTAA digit span	RHC CSF P-tau ₁₈₁ TMT-B age

Follow-up interval (in years)	Sample size MCI-AD/MCI non AD	Model	Overall classification accuracy in % (95% CI)	Sensitivity in % (95% CI)	Specificity in % (95% CI)
2-y follow up	58/72	TMT-B	64.6 (55.8, 73.5)	49.6 (35.8, 63.4)	76.2 (66.8, 85.5)
		LHC and digit span	72.2 (64.5, 79.6)	77.7 (67.7, 87.7)	68.2 (57.3, 79.2)
		LHC and LR _{TAA} and digit span	74.0 (65.8, 79.6)	83.1 (74.2, 92.1)	66.8 (56.6, 76.9)
		TMT-B, RHC and CSF P-tau ₁₈₁ /Aβ ₁₋₄₂ and age	76.3 (68.4, 84.2)	87.5 (78.9, 96.0)	68.3 (56.9, 79.6)

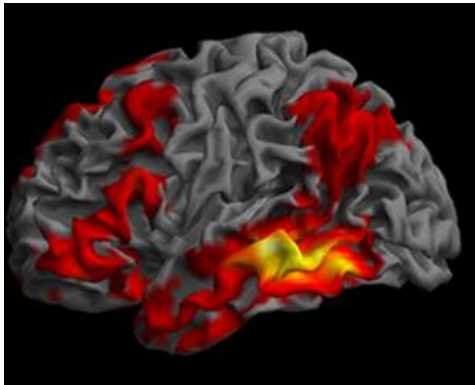
Conclusions

- None of the imaging methods used in ADNI is as accurate as a clinical diagnosis
- Single features, such as hippocampal volume are not as accurate as multiple features, such as whole brain or cortical thickness measurements.
- The best classifiers combine optimum features from different modalities including CSF biomarkers, MRI, FDG-PET, and cognitive measures, as well as factors such as age and APOE ϵ_4 allele status.
- The most discriminative measures include hippocampal volume, entorhinal cortical thickness, entorhinal metabolism, the t-tau/Ab-42 ratio, and ADAS-cog scores.
- Glucose hypometabolism alone has been shown to have high classification accuracy.
- Longitudinal data may provide even more accurate diagnoses

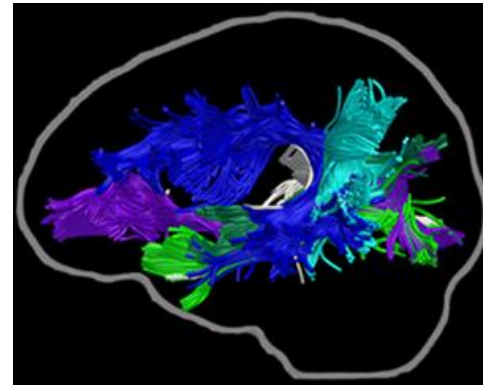
Multi-Modal Imaging Analysis

Multimodality Neuroimaging Research

- Each modality provides **unique** and potentially **complementary** information



Functional connectivity



Structural connectivity

[Turken & Dronkers, 2011]

- Most imaging studies have exploited structural or physiological alterations separately
- Power may be gained by analyzing structural and physiological alterations seen in brain together

Benefits of MMI

- Improve diagnosis sensitivity/specificity
- Determine the extent to which changes in the brain are the best predictors of the outcomes measures (e.g. diagnosis, cognitive ability, decline in cognition)
- Determine the “added information” of each modality

ROC for AD vs. HC classification

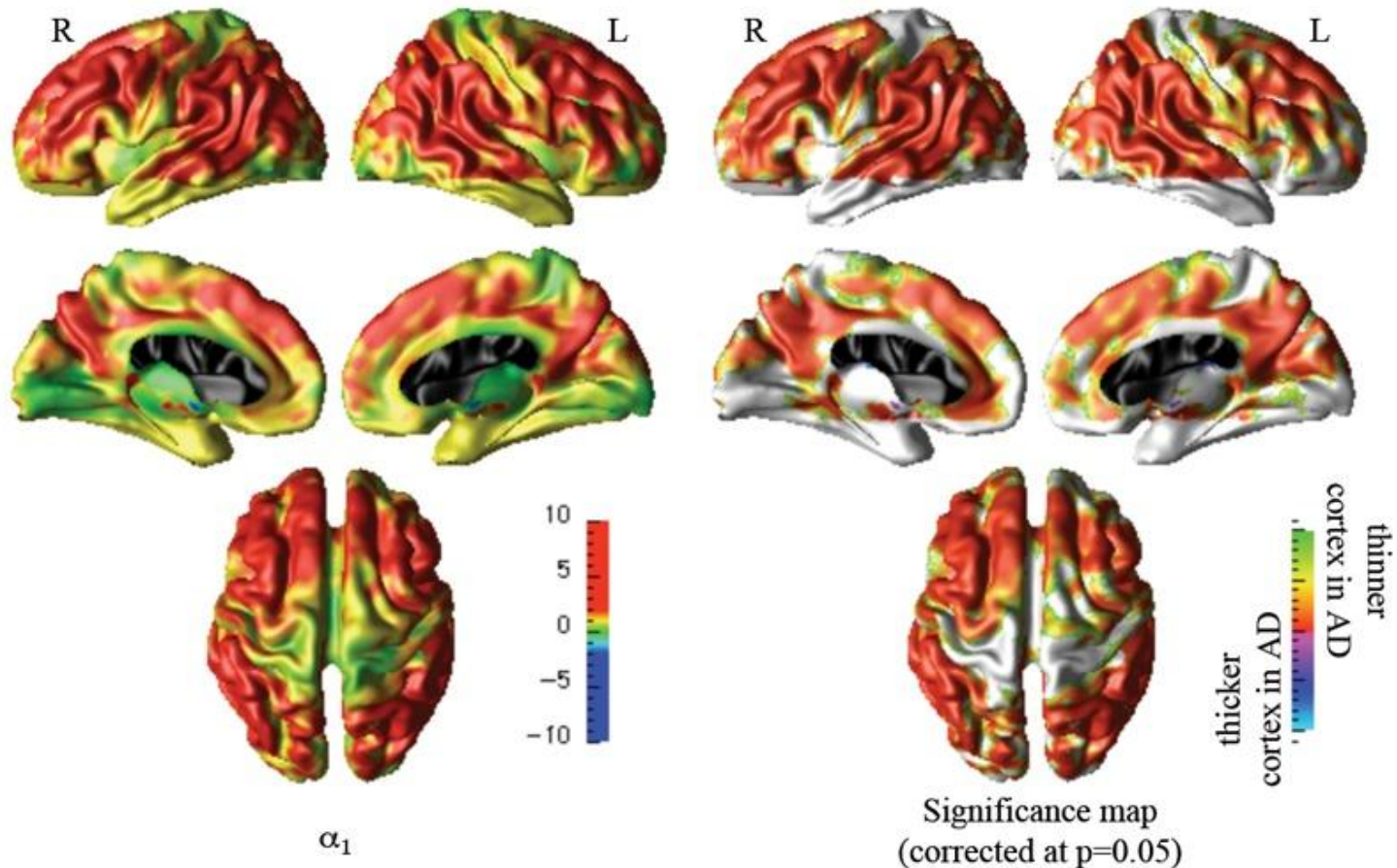
Stepwise regression analysis for the total sample with recognition (hits minus errors) as the dependent variable

	β	p	R^2	F	Model p
Total sample					
Model I					
MR Hippocampus	.47	.000	.22	44.850	.000
Model II					
MR Hippocampus	.47	.000			
PET Hippocampus	.28	.000	.30	33.890	.000
Model III					
MR Hippocampus	.40	.000			
PET Hippocampus	.29	.000			
MR Parahippocampal cortex	.17	.018	.33	25.160	.000
Model IV					
MR Hippocampus	.34	.000			
PET Hippocampus	.25	.000			
MR Parahippocampal cortex	.17	.018			
APOE	.15	.047	.34	20.230	.000

[Walhovd et al., NBoA 2008]

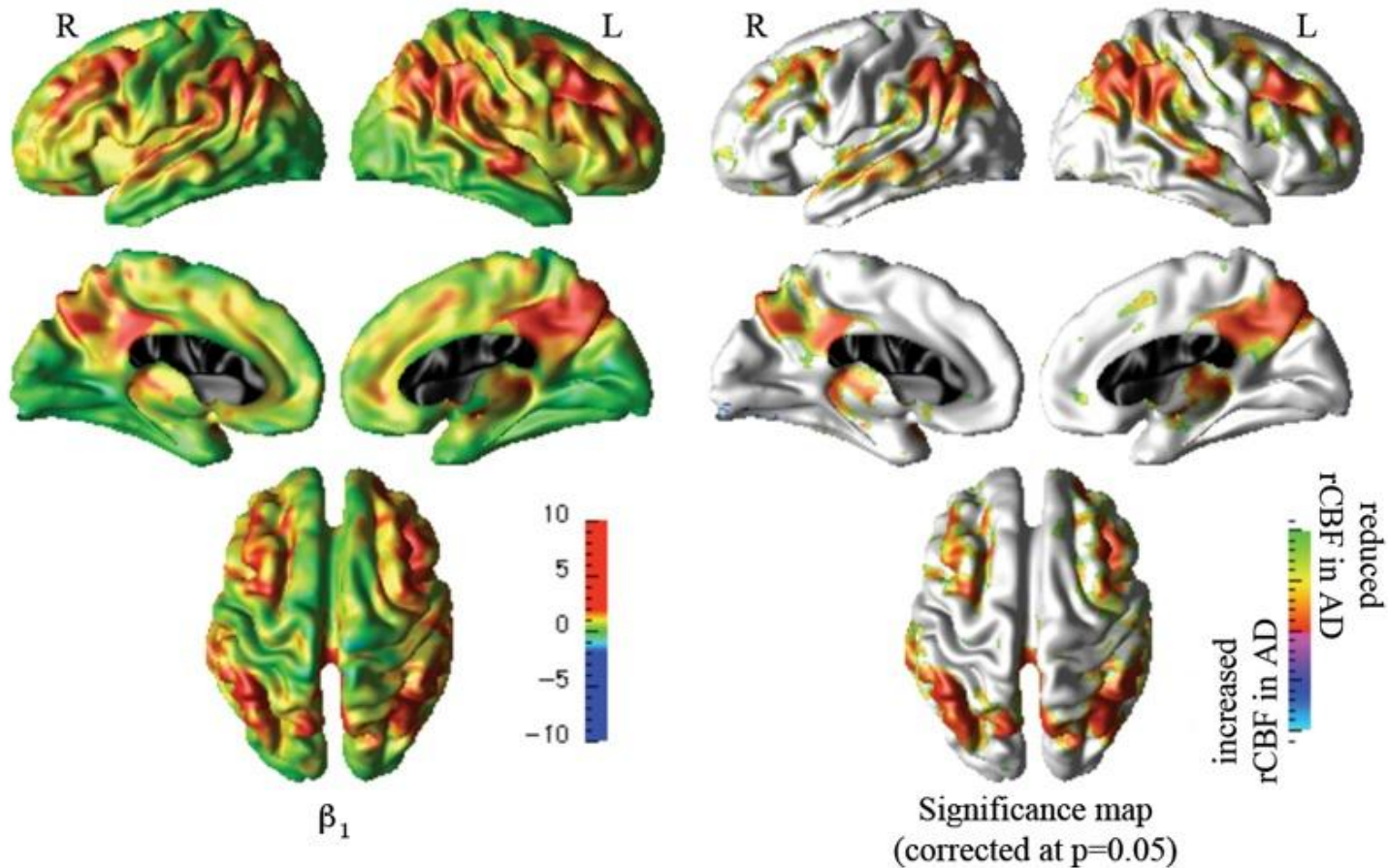
Classification Power Of Cortical Thinning

$$\log \frac{\Pr(D = AD | i)}{1 - \Pr(D = AD | i)} \sim \alpha_1 \cdot T_i$$



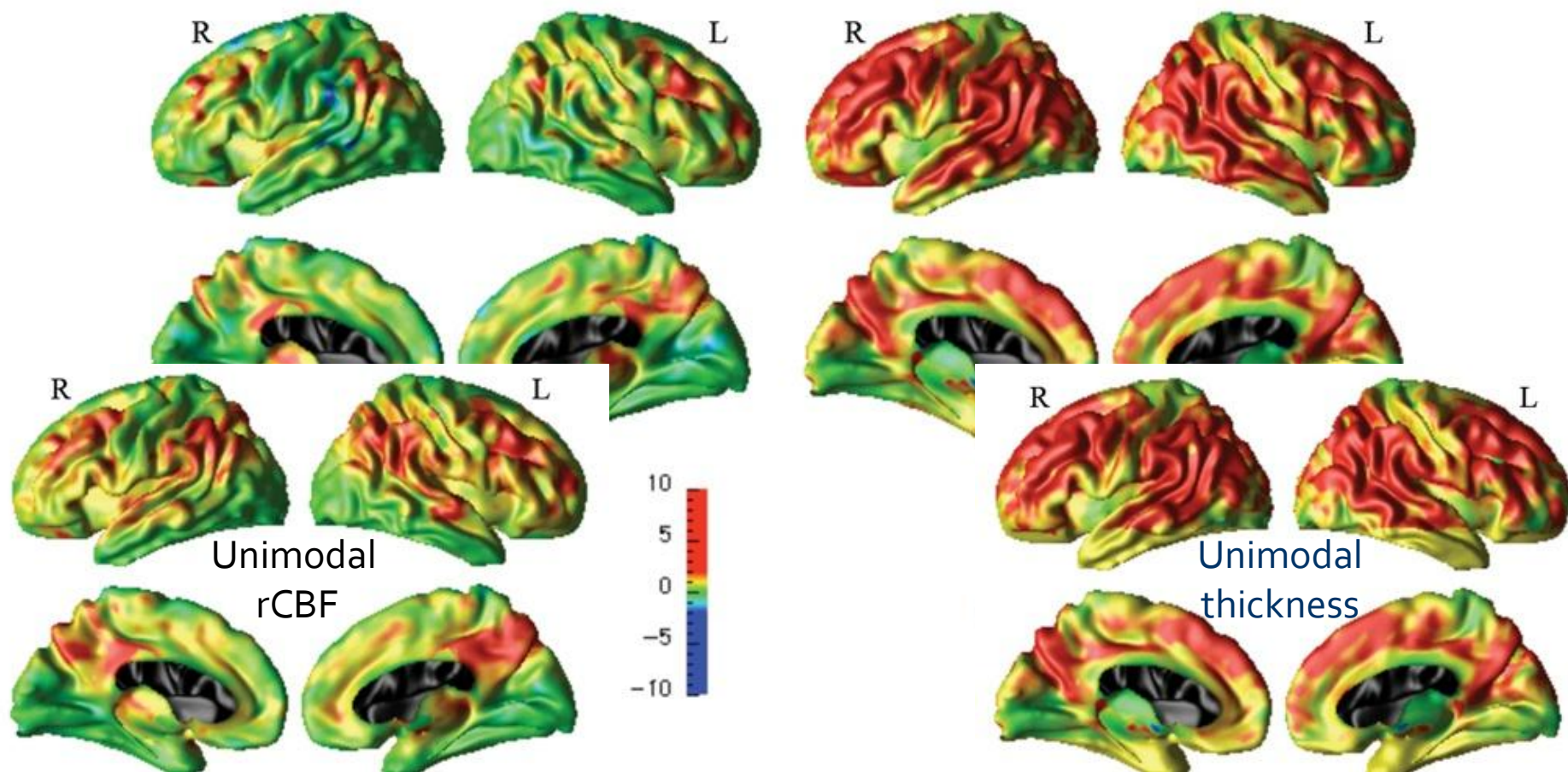
Classification Power Of Reduced rCBF

$$\log \frac{\Pr(D = AD | i)}{1 - \Pr(D = AD | i)} \sim \beta_1 \cdot P_i$$



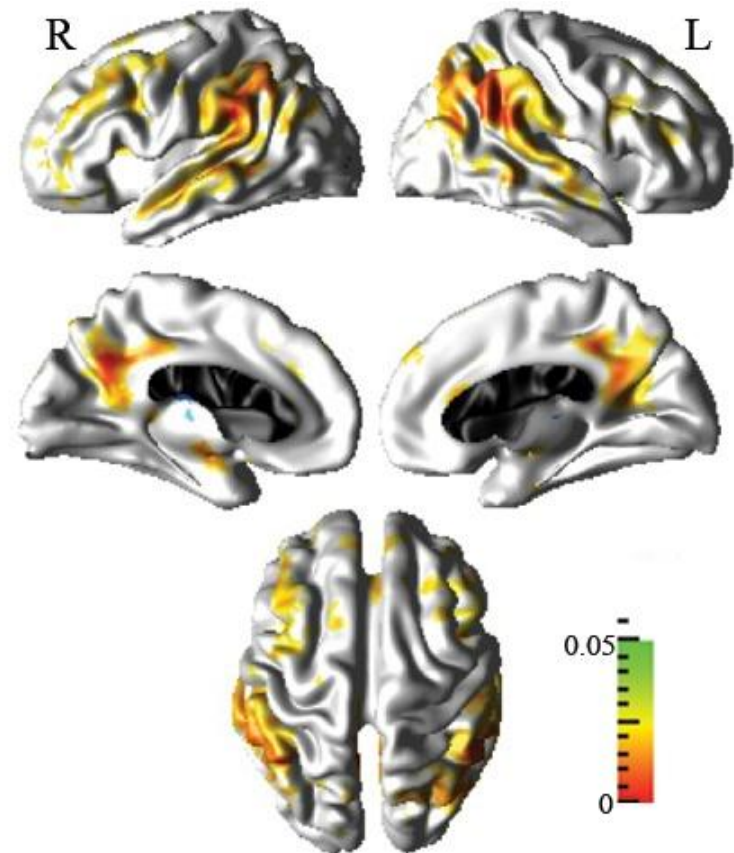
Classification Power of Cortical Thinning and rCBF in Joint Analysis

$$\log \frac{\Pr(D = AD | i)}{1 - \Pr(D = AD | i)} \sim \gamma_1 \bullet P_i + \gamma_2 \bullet T_i + \gamma_3 \bullet P_i : T_i$$



Unimodal Vs Multimodal Comparison

- Significance tested by 60-fold bootstrapping
- Cortical thinning significantly dominated reduced rCBF in power for a correct classification of AD and CN
- No cortical regions where reduced rCBF significantly dominated cortical thinning in power for a correct classification of AD and CN



The MIND Research Network, Albuquerque, NM
mialab.mrn.org/software/fit/

Fusion ICA Toolbox (FIT)

